THE JOURNAL OF BIOLOGICAL CHEMISTRY VOL. 284, NO. 17, pp. 11690–11697, April 24, 2009

Crystal Structure of Biotin Carboxylase in Complex with Substrates and Implications for Its Catalytic Mechanism*

Received for publication, July 28, 2008, and in revised form, February 9, 2009 Published, JBC Papers in Press, February 12, 2009, DOI 10.1074/jbc.M805783200

Chi-Yuan Chou[‡§1], **Linda P. C. Yu**[‡], **and Liang Tong**[‡2]

From the [‡]*Department of Biological Sciences, Columbia University, New York, New York 10027 and the* [§]*Department of Life Sciences and Institute of Genome Sciences, National Yang-Ming University, Taipei 112, Taiwan*

Biotin-dependent carboxylases are widely distributed in nature and have important functions in many cellular processes. These enzymes share a conserved biotin carboxylase (BC) component, which catalyzes the ATP-dependent carboxylation of biotin using bicarbonate as the donor. Despite the availability of a large amount of biochemical and structural information on BC, the molecular basis for its catalysis is currently still poorly understood. We report here the crystal structure at 2.0 Å resolution of wild-type *Escherichia coli* BC in complex with its substrates biotin, bicarbonate, and Mg-ADP. The structure suggests that Glu^{296} is the general base that extracts the proton from bicarbonate, and Arg^{338} is the residue that stabilizes the enolate biotin intermediate in the carboxylation reaction. The B domain of BC is positioned closer to the active site, leading to a 2-Å shift in the bound position of the adenine nucleotide and bringing it near the bicarbonate for catalysis. One of the oxygen atoms of bicarbonate is located in the correct position to initiate the nucleophilic attack on ATP to form the carboxyphosphate intermediate. This oxygen is also located close to the N1′ atom of biotin, providing strong evidence that the phosphate group, derived from decomposition of carboxyphosphate, is the general base that extracts the proton on this N1′ atom. The structural observations are supported by mutagenesis and kinetic studies. Overall, this first structure of BC in complex with substrates offers unprecedented insights into the molecular mechanism for the catalysis by this family of enzymes.

Biotin-dependent carboxylases are widely distributed in nature and have important functions in fatty acid, cholesterol, and amino acid metabolism, gluconeogenesis, insulin secretion, and other cellular processes. These enzymes include acetyl-CoA carboxylase (ACC)[3] (1–3), propionyl-CoA carboxylase (4, 5), methylcrotonyl-CoA carboxylase (6), and pyruvate carboxylase (7), and they have significant implications for human health. Mutations in propionyl-CoA carboxylase, methylcrotonyl-CoA carboxylase, and pyruvate carboxylase are linked to serious human diseases, such as propionic acidemia, lactic acidosis, and mental retardation, and the ACCs are attractive targets for the development of new therapeutic agents against diabetes, obesity, and other manifestations of the metabolic syndrome (8–10).

The biotin-dependent carboxylases generally contain three components: a biotin carboxylase (BC) activity that produces an activated carboxyl group covalently attached to biotin, a carboxyltransferase activity that transfers the carboxyl group to the acceptor molecule (acetyl-CoA, propionyl-CoA, pyruvate, and others), and a biotin carboxyl carrier protein (BCCP) that carries the biotin group, linked covalently to the side chain of a lysine residue. The carboxyltransferase component can differ greatly in sequence and structure, depending on the identity of the acceptor molecule for the carboxyl group. For example, there is no similarity between the carboxyltransferase components of ACC and pyruvate carboxylase (11–14). On the other hand, the BC activity is shared among all of these enzymes, and the BC components have significant amino acid sequence homology.

BC catalyzes the ATP-dependent carboxylation of biotin, and bicarbonate is the donor of the carboxyl group in this reaction (15, 16). This activity has been studied extensively over the years by kinetic and mutagenesis experiments, and structural information is available on the free enzyme and ATP complex of BC from several different carboxylases (13, 14, 17–24). The structure of BC contains three domains, the A, B, and C domains, and the active site is located at the interface between the B domain and the other two domains (Fig. 1*A*). Bacterial BC is a stable dimer (Fig. 1*A*), with an extensive, although rather hydrophilic, interface (21). In comparison, the BC component of eukaryotic ACC is monomeric in solution and is catalytically inactive (19, 25).

Despite this large body of knowledge on BC, the binding modes of the biotin and bicarbonate substrates to this enzyme are still not known, and therefore the molecular basis for its catalysis is currently still poorly understood. We report here the crystal structure at 2.0 Å resolution of wild-type BC from *Escherichia coli* in complex with biotin, bicarbonate, and Mg-ADP. This first structure of BC in complex with its substrates offers unprecedented insights into the molecular mechanism for the catalysis by this family of enzymes.

MATERIALS AND METHODS

Crystals of wild-type *E. coli* BC in complex with biotin, bicarbonate, and Mg-ADP were obtained at room temperature by

* This work was supported, in whole or in part, by National Institutes of Health Grant DK067238 (to L. T.).

The atomic coordinates and structure factors (codes 3G8C and 3G8D) have been deposited in the Protein Data Bank, Research Collaboratory for Structural Bioinformatics, Rutgers University, New Brunswick, NJ (http://www.rcsb.org/).

[1] Supported by Taiwan National Science Council Grants NSC-095-SAF-I-564-608-TMS and NSC-97–2314-B-010-058.

[2] To whom correspondence should be addressed. Tel.: 212-854-5203; E-mail: ltong@columbia.edu.

[3] The abbreviations used are: ACC, acetyl-CoA carboxylase; BC, biotin carboxylase; BCCP, biotin carboxyl carrier protein; r.m.s., root mean square; AMP-PNP, 5′-adenylyl-β,γ-imidodiphosphate; CPS, carbamoyl phosphate synthetase.

the sitting drop vapor diffusion method. The protein solution was at 10 mg/ml concentration, which also included 5 mM Mg-ADP, 100 mM biotin, 20 mM bicarbonate, and 3.9% (w/v) sorbitol as an additive. The reservoir solution contained 23% (w/v) polyethylene glycol 3350 and 0.12 M Li_2SO_4. Crystals were soaked overnight in a solution of 2.5 mM Mg-ADP, 200 mM biotin, 10 mM bicarbonate, 23% (w/v) polyethylene glycol 3350, 0.05 M Li_2SO_4, and 2.1% (w/v) sorbitol, cryo-protected in this solution supplemented with 12% (v/v) glycerol, and flash-frozen in liquid nitrogen.

X-ray diffraction data were collected at 100 K at the National Synchrotron Light Source beamline X4C on a Mar CCD (x-ray wavelength 0.979 Å). The diffraction images were processed and scaled with the HKL package (26). The crystal belongs to space group $P2_12_12_1$, with cell parameters of $a = 83.3$ Å, $b = 106.2$ Å, and $c = 121.5$ Å. There is a dimer in the asymmetric unit.

The structure was solved by the molecular replacement method with the program Phaser (27), using the structure of the ATP complex of the E288K mutant of BC (Protein Data Bank code 1DV2) as the search model (18). Manual rebuilding of the structure model was performed with O (28), and structure refinement was carried out with the programs CNS (29) and Refmac (30). The data processing and refinement statistics are summarized in Table 1.

The E296A and R338A mutants of BC were produced by using the QuikChange kit (Stratagene) and verified by DNA sequencing. The enzyme activity of the wild-type and mutant BC was determined spectrophotometrically at 340 nm, following a published protocol (31). The reaction mixture contained 100 mM HEPES (pH 8.5), 0.5 mM ATP, 8 mM $MgCl_2$, 40 mM biotin, 0.2 mM NADH, 0.5 mM phosphoenolpyruvate, 7 units of lactate dehydrogenase, 4.2 units of pyruvate kinase, and varying concentrations of bicarbonate. For assays that varied biotin concentration, the reaction mixture contained 100 mM HEPES (pH 7.4), 0.5 mM ATP, 8 mM $MgCl_2$, 40 mM bicarbonate, 0.2 mM NADH, 0.5 mM phosphoenolpyruvate, 7 units of lactate dehydrogenase, and 4.2 units of pyruvate kinase. To maintain the ionic strength of the solution, KCl was added to make the total concentration of biotin and KCl 200 mM.

The amount of carboxybiotin produced by BC was determined by a ^{14}C bicarbonate fixation assay (31). The reaction was carried out in a total volume of 0.5 ml at 25 °C. The mixture contained 5 mM ATP, 8 mM $MgCl_2$, 100 mM biotin, 70 mM $KHCO_3$, 100 mM HEPES (pH 8.0), and 3.5 μl (0.875 nCi) of an $NaH^{14}CO_3$ solution. The reaction was initiated by the addition of enzyme. After 1 h of incubation, the reaction was stopped by the addition of 3.6 μl of a saturated KOH solution. Then 200 μl of a 2.0 M $BaCl_2$, 0.1 M $Ba(OH)_2$ solution were added to precipitate the carbonate. The tubes were mixed and sat for 2 min and then were centrifuged at 13,000 rpm for 5 min. A 100-μl aliquot from the supernatant was transferred to a scintillation vial containing 3 ml of scintillation mixture and counted by a liquid scintillation analyzer (TRI-Carb 2900TR; PerkinElmer).

The amount of ADP produced was measured to determine the stoichiometry of carboxybiotin and ADP formation. The reaction was the same as that for the carboxybiotin assay except that no ^{14}C bicarbonate was added. Upon mixing the reaction components, an aliquot of 100 μl was removed immediately and after a 1-h incubation. The amount of ATP in each aliquot was measured by end point analysis, in a total volume of 1.0 ml with 10 units of hexokinase, 5 units of glucose-6-phosphate dehydrogenase, 0.5 mM glucose, 0.4 mM $NADP^+$, 8 mM $MgCl_2$, and 100 mM HEPES (pH 8.0). The amount of ADP produced was determined from the difference between the amount of ATP at the beginning and after the 1-h incubation.

TABLE 1
Summary of crystallographic information

Protein	Wild-type BC	E296A mutant
Space group	$P2_12_12_1$	$P2_12_12_1$
Cell parameters, *a*, *b*, *c* (Å)	83.3, 106.2, 121.5	81.3, 114.7, 122.2
Resolution[a] (Å)	30-2.0 (2.07-2.00)	30-1.9 (1.97-1.90)
R_{merge} (%)	6.3 (34.3)	6.9 (37.0)
$I/\sigma I$	21.6 (4.3)	26.2 (5.2)
Completeness (%)	99 (100)	100 (100)
No. of reflections	69,308	86,281
R factor (%)	18.2 (19.2)	19.8 (21.3)
Free *R* factor (%)	21.6 (25.0)	22.6 (25.9)
r.m.s. deviation in bond length (Å)	0.009	0.009
r.m.s. deviation in bond angles (degrees)	1.2	1.1

[a] The numbers in parentheses are for the highest resolution shell.

Crystals of the E296A mutant were obtained by the sitting drop vapor diffusion method at room temperature. The crystallization condition was essentially the same as that for the wild-type BC, and the crystal was soaked overnight in a solution containing 2.5 mM Mg-ADP, 200 mM biotin, 10 mM bicarbonate, 23% (w/v) polyethylene glycol 3350, 0.05 M Li_2SO_4, and 2.1% (w/v) sorbitol. X-ray diffraction data were collected at the X29A beamline at the National Synchrotron Light Source. The structure was solved with the program COMO (32), and the structure refinement followed the protocol described above for the wild-type enzyme. The crystallographic statistics are summarized in Table 1.

RESULTS AND DISCUSSION

Overall Structure of BC in Complex with Substrates—To ensure the binding of the biotin and bicarbonate substrates, we included high concentrations of both compounds (100 and 20 mM, respectively) as well as 5 mM Mg-ADP in the co-crystallization experiments. After many attempts, we were able to produce crystals of the wild-type BC from *E. coli* in complex with biotin, bicarbonate, and Mg-ADP and determined its structure at 2.0 Å resolution (Table 1). The refined atomic model has excellent agreement with the crystallographic data and the expected bond lengths and bond angles. About 92% of the residues are in the most favored region of the Ramachandran plot, and none of the residues are in the disallowed region.

The two monomers of the BC dimer have essentially the same conformation (Fig. 1*A*), with r.m.s. distance of 0.25 Å between their equivalent Cα atoms (excluding residues in the B domain, which have weak electron density). The overall structure of the BC monomer in this complex is similar to other structures of *E. coli* BC reported earlier. For example, the r.m.s. distance between equivalent Cα atoms of this structure and those in the structure of the active site mutant (E288K) in complex with ATP (18) is 0.4 Å. The BC dimer in the two structures is also similar, with an r.m.s. distance of 0.45 Å. The B domain

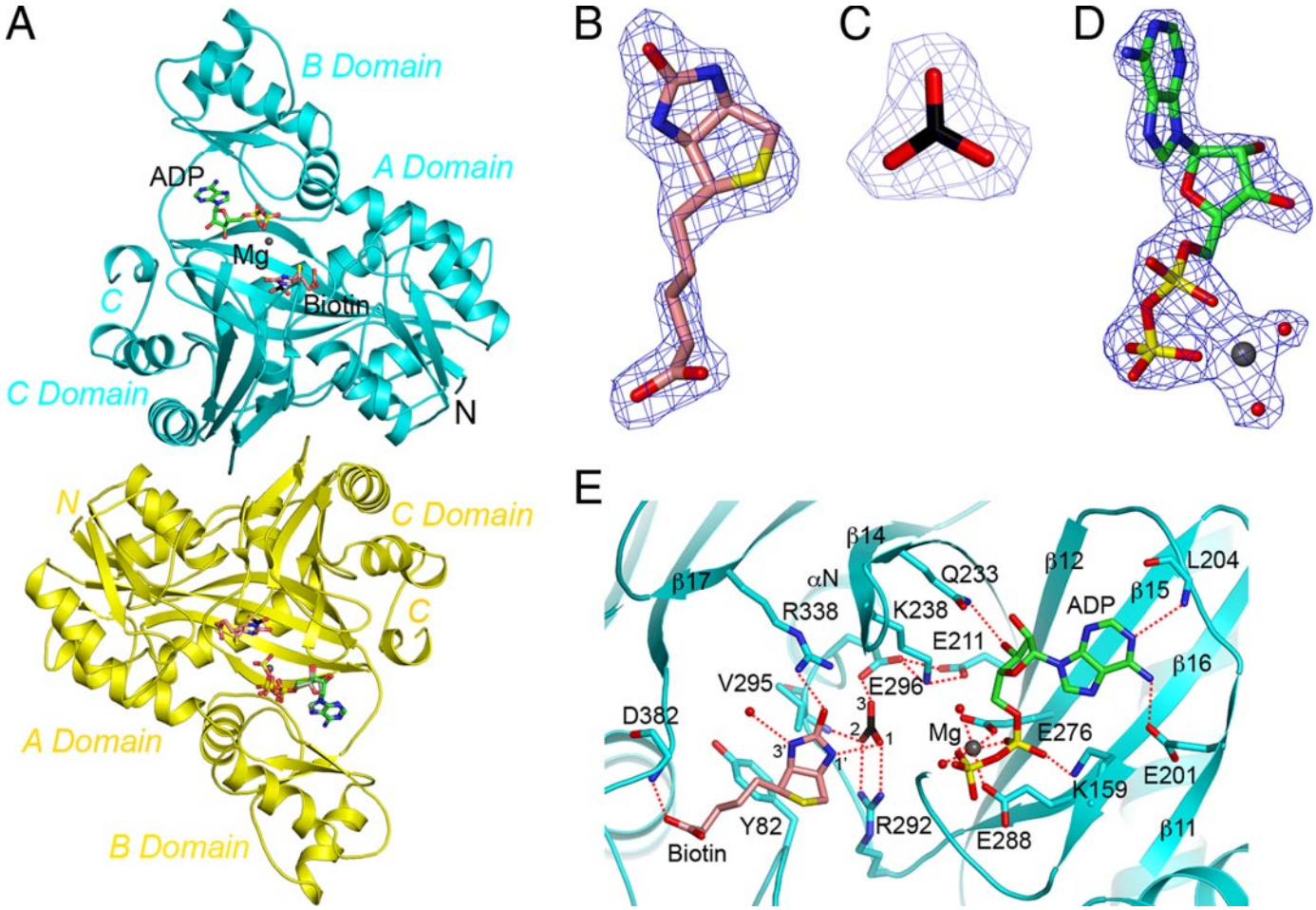

FIGURE 1. **Structure of wild-type *E. coli* BC in complex with biotin, bicarbonate, and Mg-ADP.** *A*, overall structure of the *E. coli* BC dimer in complex with the substrates. Biotin, bicarbonate, and ADP are shown in *pink*, *black*, and *green* for carbon atoms, respectively. The modeled binding mode of ATP (in *gray*) is shown for the monomer in *yellow* (PDB 3G8C). *B*, final $2F_o - F_c$ electron density for biotin at 2.0 Å resolution, contoured at 1σ. The omit $F_o - F_c$ density looks essentially the same. *C*, electron density for bicarbonate. *D*, electron density for Mg-ADP. *E*, schematic drawing showing detailed interactions in the active site of BC. Hydrogen bonding and ion pair interactions are indicated with the *dashed lines* in *red*. All structure figures in this paper are produced with PyMOL (44).

has noticeable differences in its position in the two structures and is excluded from these comparisons (see below).

Binding Modes of Bicarbonate, Biotin, and Mg-ADP—The crystallographic analysis showed that biotin (Fig. 1*B*), bicarbonate (Fig. 1*C*), and Mg-ADP (Fig. 1*D*) have clearly defined electron density, suggesting that they are well ordered in the active site of BC. Two of the oxygen atoms (O1 and O2) of bicarbonate are recognized by bidentate ion pair interactions with the side-chain guanidinium group of Arg^{292} (in the β16-αN loop in the C domain), and the O2 atom also has a hydrogen-bonding interaction with the main-chain amide of Val^{295} (Fig. 1*E*). The third oxygen atom (O3) of bicarbonate is located within 2.5 Å of the side-chain carboxylate group of Glu^{296}. This oxygen therefore is likely to carry the proton of bicarbonate, and Glu^{296} probably functions as the general base during the catalysis to extract this proton from bicarbonate (see below).

Biotin is placed over the side chains of Tyr^{82} (in the A domain) and Val^{295} (in the β16-αN loop in the C domain) in the active site of BC (Fig. 1*E*). The carbonyl oxygen atom in the ureido ring has hydrogen-bonding interactions with the side chain of Arg^{338} (in strand β17 in the C domain), which also shows interactions with the bicarbonate. Unexpectedly, the structure reveals that the N1′ atom of biotin is located within 2.7 Å of the O1 atom of bicarbonate. This close approach probably helps to position the biotin group in the active site, and also has important implications for the catalysis by BC (see below). The N3′ atom of biotin is hydrogen-bonded to a water molecule. The valeric side chain of biotin is less ordered and has weaker electron density (Fig. 1*B*), and one of the carboxylate oxygen atoms is hydrogen-bonded to the main-chain amide of residue Asp^{382} (Fig. 1*E*). This interaction may also be maintained with the natural substrate of BC, BCCP-biotin, where the carboxylate group is replaced with an amide bond to a lysine residue in BCCP.

The biotin concentration used in the crystallization experiment (100 mM) is about 3-fold higher than the K_m value based on our kinetic assays (Table 2), although an earlier study suggested that the K_m for biotin is about 130 mM (31). The crystallographic analyses showed that the average temperature factor for biotin (43 $Å^2$) is comparable with that of ADP, suggesting that biotin is present in high occupancy in the active site.

The magnesium ion is coordinated by six ligands arranged in an octahedral fashion (Fig. 1*E*), including a terminal oxygen atom from the α- and β-phosphate groups of ADP, an oxygen

from the side-chain carboxylate groups of Glu^{276} (strand β15 in the C domain) and Glu^{288} (strand β16) and two water molecules. The β-phosphate cannot rotate freely for Mg^{2+} binding, which may explain the fact that positional isotope exchange was not observed in kinetic studies (15). The bound position of ADP observed here is significantly different from that of ATP bound to the E288K mutant (18) as well as that of AMPPNP bound to *Staphylococcus aureus* BC (24) (see below).

The Active Site of BC—Earlier studies showed that the B domain of BC undergoes a large movement to close over the active site upon ATP binding (18). In our structure, the B domain is placed even closer to the active site, corresponding to roughly a 7° rotation compared with that in the ATP complex (Fig. 2*A*). Even with this additional movement, the active site of BC in the current complex, especially the biotin molecule, is still exposed to the solvent (Fig. 2*B*). In the reaction with the natural BCCP-biotin substrate, BCCP may help cover up this active site, which may explain why BCCP-biotin is a much better substrate for BC than biotin alone (16). The electron density for the B domain is weaker than that for the other domains in our structure, and this conformational flexibility of the B domain could also be stabilized upon the binding of BCCP.

The further closure of the B domain in our structure has a dramatic impact on the bound position of the adenine nucleotide (Fig. 2*C*). The adenine base interacts primarily with residues in the B domain, especially a hydrogen bond between its N6 atom and the main-chain carbonyl oxygen of residue Lys^{202} (Fig. 2*C*). Due to the further closure of the B domain in our structure, this carbonyl oxygen moves by 2.2 Å as compared with that in the structure of the ATP complex (18), and the bound position of ADP is also shifted by about 2 Å relative to that of ATP (Fig. 2*C*). This further closure of the B domain brings the phosphate group of the adenine nucleotide closer to the bound position of the bicarbonate group (Fig. 2*C*) and therefore should make the BC enzyme more competent for catalysis. Residues in the glycine-rich loop (GGGGRG) in the B domain have very weak electron density, and they may become better ordered in the presence of ATP and interact with its phosphate group (18).

TABLE 2
Summary of kinetic parameters
All of the assays were repeated several times to ensure reproducibility.

Protein	K_m	k_{cat}	k_{cat}/K_m
	m_M	s^{-1}	$_M{}^{-1}\,s^{-1}$
With bicarbonate as the varying substrate			
Wild-type BC	16.2 ± 2.5	0.44 ± 0.02	27.2 ± 4.3
E296A mutant	57.5 ± 7.0	0.034 ± 0.002	0.59 ± 0.08
R338A mutant	18.9 ± 1.8	0.0019 ± 0.0001	0.10 ± 0.01
With biotin as the varying substrate			
Wild-type BC	35.1 ± 4.0	0.58 ± 0.02	16.6 ± 2.0
E296A mutant	22.7 ± 3.6	0.028 ± 0.002	1.2 ± 0.2
R338A mutant	41.8 ± 6.7	0.0025 ± 0.0001	0.06 ± 0.01

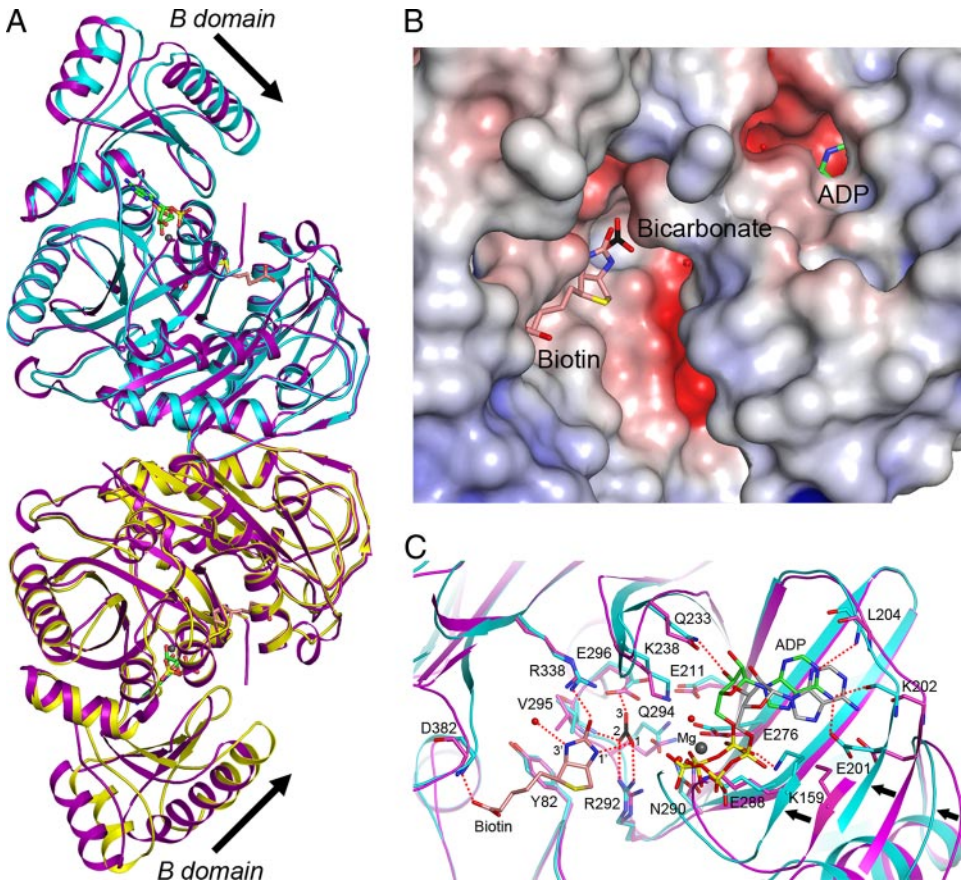

FIGURE 2. **The active site of BC.** *A*, overlay of the structure of wild-type *E. coli* BC dimer (in *cyan* and *yellow*) in complex with biotin (*pink*), bicarbonate (*black*), and Mg-ADP (*green*) with that of the E288K mutant in complex with ATP (*magenta*) (18). The conformational difference of domain B is indicated with the *arrows*. The 2-fold axis of the dimer is along the horizontal direction. *B*, molecular surface of the active site region of *E. coli* BC. The biotin molecule is exposed to the solvent. *C*, overlay of the active site region of wild-type *E. coli* BC (*cyan*) in complex with biotin, bicarbonate, and Mg-ADP with that of the E288K mutant (*magenta*) in complex with ATP (*gray*) (18). The *black arrows* indicate the further closure of the B domain in the substrate complex.

The ATP complex of *E. coli* BC was obtained with a kinetically inactive E288K mutant (18), which may have affected the conformation of the B domain and the binding mode of ATP. The structure of wild-type *S. aureus* BC in complex with AMPPNP was reported recently (24). A comparison of our structure with that complex showed that there are still differences in the conformation of the B domain, such that the positions of the adenine base and the ribose are different by about 1.3 Å between the two structures.

Compared with the structure of the ATP complex, there are only a few conformational changes in the binding sites for biotin and bicarbonate (Fig. 2*C*) (18). The largest difference is in the side chain of Gln^{294}, whose conformation in the ATP complex would clash with the bicarbonate. Smaller conformational differences are seen for the

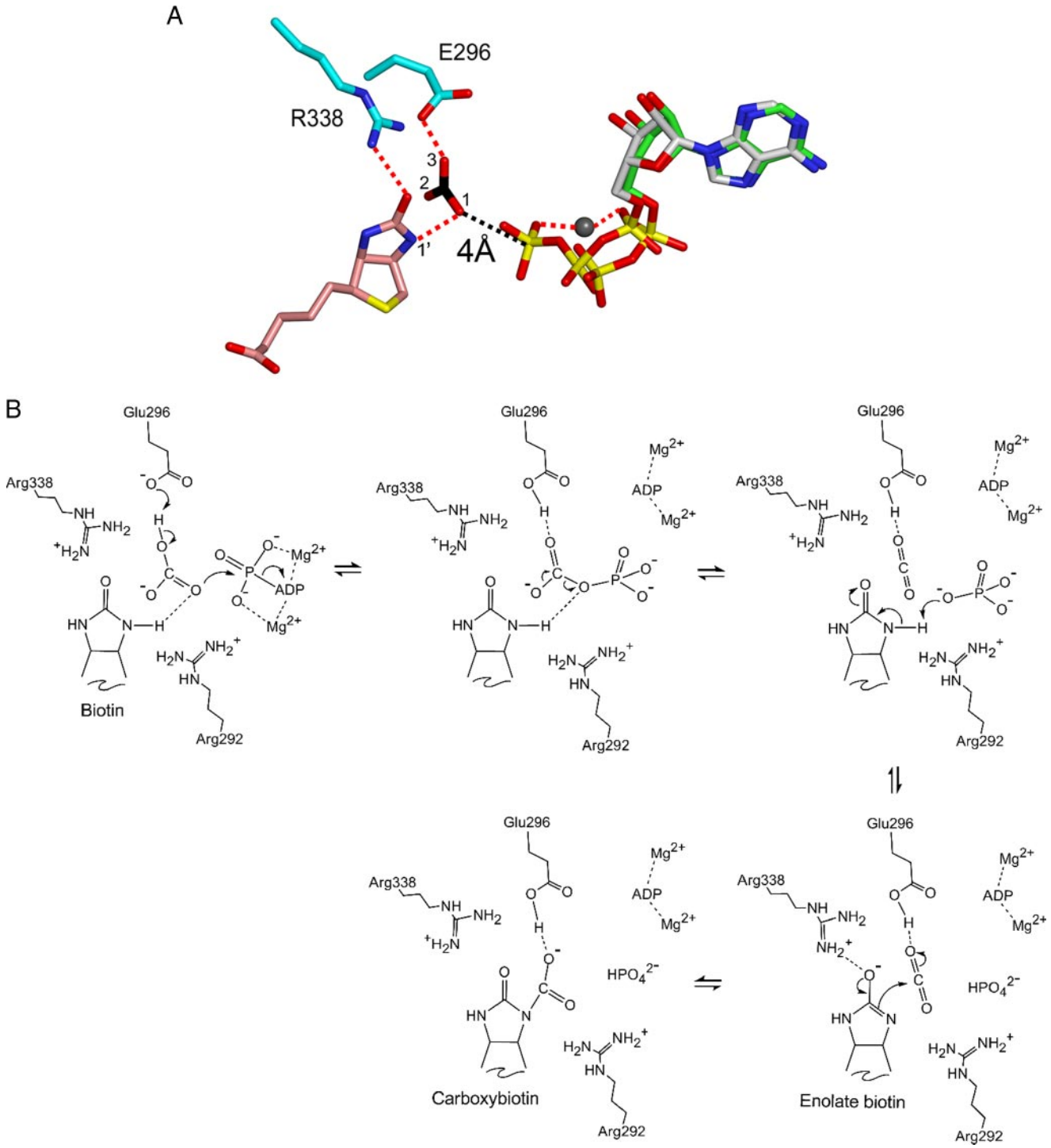

FIGURE 3. **Molecular mechanism for the catalysis by BC.** *A*, modeled binding mode of ATP (in *gray*) in the active site of BC. The bicarbonate is in the appropriate location to initiate the reaction. *B*, schematic drawing of the catalytic mechanism of BC. Glu^{296} and Arg^{338} have crucial roles in this reaction.

side chains of Asn^{290}, Arg^{292}, and Glu^{296}. On the other hand, Arg^{338} has essentially the same conformation in the two structures (Fig. 2*C*).

Molecular Basis for Catalysis by BC—To derive further insights into the catalysis by BC, we modeled the binding mode of ATP into the active site of the current structure, by manually superimposing the AMP portion of the ATP in the E288K complex (18) onto the AMP portion of ADP in our current structure. We did not make any further adjustments in the conformation of the β- and γ-phosphate groups. Modeling the binding mode of ATP based on that of AMPPNP in the *S. aureus* BC structure (24) produced a very similar result. In this model of the ATP complex, the magnesium ion is coordinated by a terminal oxygen atom from the α- and γ-phosphates (Fig. 3*A*). A second magnesium ion coordinates the β- and γ-phosphates (13, 24). After the γ-phosphate is transferred to bicar-

bonate, the two metal ions are likely to remain associated with ADP (Fig. 3*B*), one between the α- and β-phosphate (Fig. 1*E*) and one with the β-phosphate.[4]

Most importantly, the O1 atom of bicarbonate is located about 4 Å from and directly below the γ-phosphorus atom (Fig. 3*A*), suggesting that this oxygen is in the appropriate location for initiating a nucleophilic attack on the phosphorus atom. As discussed above, it is possible that an additional conformational rearrangement of the B domain can further reduce the distance between ATP and bicarbonate and thereby facilitate the catalysis. This rearrangement may also reduce the surface exposure of the active site region.

Our structural observations provide unprecedented molecular insights into the catalysis by BC. Earlier studies have suggested the presence of a carboxyphosphate intermediate, although it has not been observed experimentally for the BC reaction (15, 16). Our structure shows that the O1 atom of bicarbonate can initiate the nucleophilic attack on the γ-phosphate of ATP (Fig. 3*A*), which would lead to the formation of carboxyphosphate (Fig. 3*B*). Glu^{296} is the best candidate for the general base that deprotonates the bicarbonate. The pK_a of bicarbonate is normally 10.3, which would make it difficult for a Glu side chain to extract its proton. However, the bicarbonate interacts with several positively charged side chains of BC, including Arg^{338} and Arg^{292} (Fig. 1*E*), which should reduce its apparent pK_a value. In addition, the Glu^{296} side chain interacts with the side chain of Glu^{211} (Fig. 1*E*), which should disfavor ionization and increase the apparent pK_a of Glu^{296}. It is known from studies of other proteins that the pK_a of an acidic side chain can be >9 in special cases (33). Overall, the combined effects of the local environment of the BC active site probably make the pK_a values of Glu^{296} and bicarbonate closer to each other, facilitating the deprotonation of bicarbonate to initiate the reaction.

Decomposition of the unstable carboxyphosphate produces CO_2 and PO_4^{3-}. One of the oxygen atoms on the phosphate group is expected to be located close to the N1′ atom of biotin, since the attacking O1 atom of bicarbonate is within 2.7 Å of this N1′ atom (Fig. 1*E*). Therefore, the phosphate group is probably the general base that extracts the proton from the N1′ atom (15). This leads to the enolization of the biotin ring, and the oxyanion is stabilized by interaction with the Arg^{338} side chain (Fig. 3*B*). Finally, attack on the N1′ atom by CO_2 leads to the formation of carboxybiotin (Fig. 3*B*). Overall, the structural observations define the molecular basis for the catalysis and provide the first direct experimental evidence in support of the kinetic mechanism proposed earlier (15).

The pK_a for the proton on the N1′ atom of free biotin is 17.4 (34). The interaction between the ureido oxygen and Arg^{338} in the active site of BC is expected to reduce this pK_a value, which should facilitate the extraction of this proton by the phosphate group (the pK_a of HPO_4^{2-} is 12.7).

Mutagenesis Studies Support the Structural Observations—Our structural analyses identify Glu^{296} and Arg^{338} as two of the residues with important roles for catalysis by BC. The R338S and R338Q mutants (35), as well as mutations at a large number of other residues in the active site region of BC, have been characterized earlier (16, 31, 36, 37). On the other hand, the Glu^{296} residue has not been studied by mutagenesis experiments. We produced the E296A and R338A mutants of *E. coli* BC, and our kinetic data showed that the E296A mutant has a 45-fold loss in activity measured based on k_{cat}/K_m toward the bicarbonate substrate, as a result of a 13-fold loss in k_{cat} and 3.5-fold increase in K_m (Table 2). In comparison, the R338A mutant is essentially inactive, with a roughly 270-fold loss in activity due to a large decrease in k_{cat}. An earlier study showed that wild-type *E. coli* BC had a K_m of 0.37 mM toward the bicarbonate substrate (31), whereas the value from our study was about 20 mM, determined from many experiments (Table 2). The reasons for this difference between the two studies are not known. As a comparison, K_m values of between 3 and 13 mM for bicarbonate have been reported for mammalian ACCs (38), in the same range as our value for *E. coli* BC.

The increase in the K_m value of the E296A mutant for bicarbonate is consistent with our structure showing a direct interaction between the Glu^{296} side chain and bicarbonate (Fig. 1*E*). The relatively smaller loss in the k_{cat} of this mutant is probably due to a hydroxide ion mimicking the effects of the Glu side chain, since the Glu^{296} residue is involved in a network of hydrogen bonds (Fig. 1*E*). Our earlier studies with human cytomegalovirus protease showed the presence of a solvent molecule when the third member of the catalytic triad (His^{157}) was mutated to Ala (39).

To obtain direct evidence for this hydroxide ion, we have determined the crystal structure of the E296A mutant at 1.9 Å resolution (Table 1 and Fig. 4*A*). The structure clearly showed that a solvent molecule (possibly a hydroxide ion) occupies the same position as that of the carboxylate oxygen atom in the Glu^{296} side chain that is hydrogen-bonded to the bicarbonate (Fig. 4*B*). Therefore, this hydroxide ion is in the correct position for catalysis, enabling it to partly rescue the activity of the mutant. The hydroxide is sequestered by hydrogen bonding to the main-chain amide of residue 296 and the side chains of Glu^{241} and Arg^{338}. It also interacts with a sulfate group, from the reservoir solution, which occupies the position of the bicarbonate in the wild-type BC structure (Fig. 4*B*). Strong electron density for Mg-ADP is observed in the active site of one of the monomers, whereas no electron density for Mg-ADP is observed in the other active site of the dimer (Fig. 4*A*). Consistent with this, the B domain of the other monomer also has much weaker electron density, and residues 133–203 in this domain are not included in the current atomic model.

Our kinetic results on the R338A mutant are consistent with those on the R338Q and R338S mutants reported earlier (35). The R338A and R338Q mutants have roughly the same K_m toward biotin as the wild-type enzyme, suggesting that this residue may not be essential for biotin binding. On the other hand, these mutants have a more than 100-fold loss in k_{cat}, consistent with the hypothesis that Arg^{338} may be important for stabilizing the enolate biotin transition state intermediate. The R338Q and R338S mutants also showed a 50-fold increase in the K_m for ATP (35), and further studies are needed to understand the molecular basis for this change. The Arg^{338} residue of *E. coli* BC

[4] C.-Y. Chou and L. Tong, unpublished results.

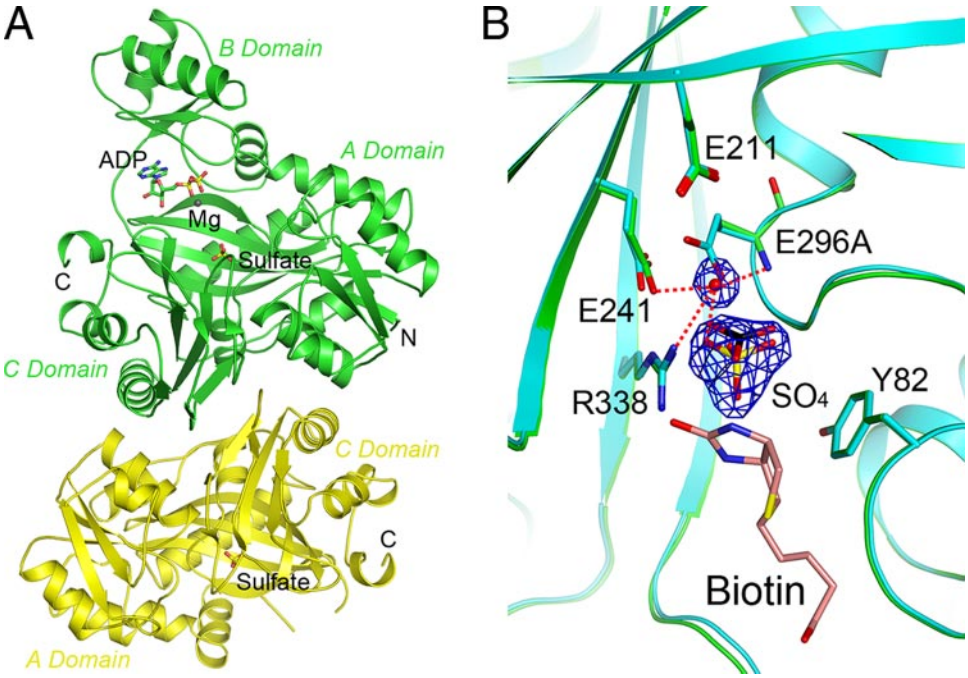

FIGURE 4. **Structure of the E296A mutant of *E. coli* BC.** *A*, overall structure of the E296A dimer in complex with Mg-ADP and sulfate. Residues 133–203 in the B domain of the monomer in *yellow* are not included in the current atomic model due to disorder (PDB 3G8D). *B*, overlay of the active site region of the E296A mutant (in *green*) with that of the wild-type BC (in *cyan*). Final $2F_o - F_c$ electron density at 1.9 Å resolution is shown for the water and sulfate, contoured at 1σ. The bound positions of bicarbonate and biotin in the wild-type BC structure are also shown.

	80 85	270 280 290 300 335 340
		β15 β16 αN
E. coli BC	PGYGFL	RGAGTFEFLFE...NGEFYFIEMNTRIQVEHPVTEMITG VECRIN
Yeast ACC	AGWGHA	VSAGTVEYLYSH.DDGKFYFLELNPRLQVEHPTTEMVSG TACRIT
Wheat ACC	PGWGHA	VGAATVEYLYSM.ETGEYYFLELNPRLQVEHPVTEWIAE VAVRIT
Human ACC1	AGWGHA	VSAGTVEYLYSQ..DGSFYFLELNPRLQVEQPCTEMVAD IAARIT
S. coelicolor PCC	PGYGFL	RGAGTVEFIVPGSDPSQYYFMEMNTRLQVEHPVTELVTG IEARLC
Human PCC	PGYGFL	SSAGTVEFLVDS..KKNFYFLEMNTRLQVEHPVTECITG VECRVY
Rice MCC	PGYGFL	YSAGTVEFIVDT.LSGEFYFMEMNTRLQVEHPVTEMIVG FEARIY
Mouse MCC	PGYGFL	VGAGTVEFIMDS..RHNFYFMEMNTRLQVEHPVTEMITG FEARIY
Human MCC	PGCGFL	VGAGTVEFIMDS..KHNFCFMEMNTRLQVEHPVTEMITG FEARIY
S. aureus PC	PGYGFL	VNAGTVEFLVS...GDEFFFIEVNPRVQVEHTITEMVTG IQCRIT
Yeast PYC1	PGYGFL	RNAGTAEFLVDN..QNRHYFIEINPRIQVEHTITEEITG IQCRIT
Human PC	PGYGFL	ENAGTVEFLVDR..HGKHYFIEVNSRLQVEHTVTEEITD IQCRVT
E. coli CPS	mgGQTA	tggsnVQFAvnpk.ngrLIVIEMNPR.VSrssalaskat ------

FIGURE 5. **Conservation of substrate binding residues in BC.** Shown is an amino acid sequence alignment of residues that are important for binding biotin (*magenta* and *red*), bicarbonate (*red*), and Mg-ADP (*blue*), for the BC components of ACC, propionyl-CoA carboxylase (*PCC*), methylcrotonyl-CoA carboxylase (*MCC*), and pyruvate carboxylase (*PC*) from several organisms. Residues involved in binding biotin and bicarbonate are not conserved in *E. coli* CPS (43). The residues in CPS are shown in *capital letters* if they are structurally equivalent to those in BC. Residues near Arg^{338} of *E. coli* BC do not have structural equivalents in CPS (indicated with *dashes*).

is equivalent to an Arg residue in propionyl-CoA carboxylase and methylcrotonyl-CoA carboxylase, whose mutation is linked to diseases in humans (35).

Earlier studies of BC have shown that mutation of active site residues could cause a misalignment of the substrates, such that ATP hydrolysis is no longer coupled to biotin carboxylation (31, 35). We determined the ratio of ATP hydrolysis to carboxybiotin formation for wild-type BC and the E296A and R338A mutants. The ratio is 1.08 for the wild-type enzyme, suggesting good coupling between the two steps of the catalysis. For the E296A and R338A mutants, the ratio is 2.5 and 6.2, respectively, suggesting a decoupling between the two steps. The ratio for the R338A mutant is similar to that observed earlier for the R338Q and R338S mutants (35). Therefore, the loss in the overall biotin carboxylase activity of the E296A and R338A mutants is larger than the values presented in Table 2, which are determined from monitoring ATP hydrolysis. The larger ratio for the Arg^{338} mutants than for the Glu^{296} mutant may be consistent with the importance of Arg^{338} in stabilizing the transition-state of the biotin carboxylation step.

For both the E296A and R338A mutants, the possibility exists that some of the observed activity could be due to the endogenous wild-type *E. coli* BC, co-purifying with the His-tagged mutant protein by forming a heterodimer with it. However, the mutant proteins were highly overexpressed, producing about 20–30 mg of purified protein/liter of *E. coli* culture, which should minimize the amount of heterodimers with endogenous BC in the purified sample. Moreover, earlier studies have shown that a heterodimer containing one wild-type BC monomer and one inactive, mutant BC monomer is essentially inactive (40). Therefore, the contribution of the endogenous BC to the activity of both mutants is probably very small (if any).

Mutations of other residues in the active site region have also been shown to have deleterious effects. These studies demonstrate the functional importance of Glu^{211}, Lys^{238}, Asn^{290}, and Arg^{292} in the biotin and bicarbonate binding region (Fig. 1*E*) (31, 36) as well as residues in the ATP binding region (18, 37). Overall, our structural observations are consistent with and can explain these results from the mutagenesis and kinetic studies.

Implications for Catalysis by Related Enzymes—The BC component is shared among most of the biotin-dependent carboxylases. The residues that play important roles in substrate binding and/or catalysis as identified from this structure are strictly conserved among these enzymes (Fig. 5). The two residues that have van der Waals interactions with biotin (Tyr^{82} and Val^{295}) are also highly conserved. Tyr^{82} has a conservative substitution to Trp in the eukaryotic ACCs, and human methylcrotonyl-CoA carboxylase is the only enzyme that contains a Cys residue at this position (Fig. 5). Overall,

our structure of the substrate complex of *E. coli* BC is likely to have strong implications for the catalysis by these other enzymes, and they probably have conserved substrate binding modes and catalytic mechanisms.

BC belongs to the ATP-grasp superfamily of enzymes, which catalyzes the ATP-dependent formation of an amide bond between a carboxylate compound and an amine compound (41, 42). These enzymes share a similar overall fold and similar binding modes for ATP. However, the chemical identities of their carboxylate and amine substrates are highly divergent, and the sequence and structural conservation for the binding sites of these substrates is much lower. For example, the residues that are important for binding biotin in BC are not conserved in *E. coli* carbamoyl phosphate synthetase (CPS; Fig. 5) (43). On the other hand, Arg^{292} of BC is conserved in CPS and many other members of this superfamily (42), suggesting that this residue could have a conserved role in recognizing the carboxylate group in the substrate. Although CPS also uses bicarbonate as the CO_2 donor, the general base of BC, Glu^{296}, is not conserved in CPS (Fig. 5). In fact, there is a large conformational difference between BC and CPS near this residue (Fig. 5), such that the bicarbonate binding site in BC does not exist in CPS. Bicarbonate in BC actually clashes with the Ser^{304} residue in CPS, suggesting that this substrate may have a different binding mode to CPS. Further studies are needed to identify the general base in this enzyme. In summary, our crystal structure has provided the first molecular insights into the catalysis by the *E. coli* BC enzyme as well as the BC component of most biotin-dependent carboxylases.

Acknowledgments—We thank R. Abramowitz and J. Schwanof for setting up the X4C beamline and N. Whalen for setting up the X29A beamline at the National Synchrotron Light Source, W. W. Cleland for helpful discussions, and C. Huang for careful reading of the manuscript.

REFERENCES

1. Wakil, S. J., Stoops, J. K., and Joshi, V. C. (1983) *Ann. Rev. Biochem.* **52,** 537–579
2. Cronan, J. E., Jr., and Waldrop, G. L. (2002) *Prog. Lipid Res.* **41,** 407–435
3. Tong, L. (2005) *Cell. Mol. Life Sci.* **62,** 1784–1803
4. Desviat, L. R., Perez, B., Perez-Cerda, C., Rodriguez-Pombo, P., Clavero, S., and Ugarte, M. (2004) *Mol. Genet. Metab.* **83,** 28–37
5. Jiang, H., Rao, K. S., Yee, V. C., and Kraus, J. P. (2005) *J. Biol. Chem.* **280,** 27719–27727
6. Desviat, L. R., Perez-Cerda, C., Perez, B., Esparza-Gordillo, J., Rodriguez-Pombo, P., Penalva, M. A., Rodriguez de Cordoba, S., and Ugarte, M. (2003) *Mol. Genet. Metab.* **80,** 315–320
7. Jitrapakdee, S., and Wallace, J. C. (1999) *Biochem. J.* **340,** 1–16
8. Abu-Elheiga, L., Matzuk, M. M., Abo-Hashema, K. A. H., and Wakil, S. J. (2001) *Science* **291,** 2613–2616
9. Harwood, H. J., Jr. (2005) *Expert Opin. Ther. Targets* **9,** 267–281
10. Tong, L., and Harwood, H. J., Jr. (2006) *J. Cell. Biochem.* **99,** 1476–1488
11. Zhang, H., Yang, Z., Shen, Y., and Tong, L. (2003) *Science* **299,** 2064–2067
12. Hall, P. R., Zheng, R., Antony, L., Pustai-Carey, M., Carey, P. R., and Yee, V. C. (2004) *EMBO J.* **23,** 3621–3631
13. St. Maurice, M., Reinhardt, L., Surinya, K. H., Attwood, P. V., Wallace, J. C., Cleland, W. W., and Rayment, I. (2007) *Science* **317,** 1076–1079
14. Xiang, S., and Tong, L. (2008) *Nat. Struct. Mol. Biol.* **15,** 295–302
15. Knowles, J. R. (1989) *Annu. Rev. Biochem.* **58,** 195–221
16. Attwood, P. V., and Wallace, J. C. (2002) *Acc. Chem. Res.* **35,** 113–120
17. Waldrop, G. L., Rayment, I., and Holden, H. M. (1994) *Biochemistry* **33,** 10249–10256
18. Thoden, J. B., Blanchard, C. Z., Holden, H. M., and Waldrop, G. L. (2000) *J. Biol. Chem.* **275,** 16183–16190
19. Shen, Y., Volrath, S. L., Weatherly, S. C., Elich, T. D., and Tong, L. (2004) *Mol. Cell* **16,** 881–891
20. Kondo, S., Nakajima, Y., Sugio, S., Yong-Biao, J., Sueda, S., and Kondo, H. (2004) *Acta Crystallogr. Sect. D* **60**, 486–492
21. Shen, Y., Chou, C.-Y., Chang, G.-G., and Tong, L. (2006) *Mol. Cell* **22,** 807–818
22. Kondo, S., Nakajima, Y., Sugio, S., Sueda, S., Islam, M. N., and Kondo, H. (2007) *Acta Crystallogr. Sect. D* **63**, 885–890
23. Cho, Y. S., Lee, J. I., Shin, D., Kim, H. T., Cheon, Y. H., Seo, C. I., Kim, Y. E., Hyun, Y. L., Lee, Y. S., Sugiyama, K., Park, S. Y., Ro, S., Cho, J. M., Lee, T. G., and Heo, Y. S. (2007) *Proteins* **70,** 268–272
24. Mochalkin, I., Miller, J. R., Evdokimov, A., Lightle, S., Yan, C., Stover, C. K., and Waldrop, G. L. (2008) *Protein Sci.* **17,** 1706–1718
25. Weatherly, S. C., Volrath, S. L., and Elich, T. D. (2004) *Biochem. J.* **380,** 105–110
26. Otwinowski, Z., and Minor, W. (1997) *Methods Enzymol.* **276,** 307–326
27. McCoy, A. J., Grosse-Kunstleve, R. W., Storoni, L. C., and Read, R. J. (2005) *Acta Crystallogr. Sect. D* **61**, 458–464
28. Jones, T. A., Zou, J. Y., Cowan, S. W., and Kjeldgaard, M. (1991) *Acta Crystallogr. Sect. A* **47**, 110–119
29. Brunger, A. T., Adams, P. D., Clore, G. M., DeLano, W. L., Gros, P., Grosse-Kunstleve, R. W., Jiang, J.-S., Kuszewski, J., Nilges, M., Pannu, N. S., Read, R. J., Rice, L. M., Simonson, T., and Warren, G. L. (1998) *Acta Crystallogr. Sect. D* **54**, 905–921
30. Murshudov, G. N., Vagin, A. A., and Dodson, E. J. (1997) *Acta Crystallogr. Sect. D* **53**, 240–255
31. Blanchard, C. Z., Lee, Y. M., Frantom, P. A., and Waldrop, G. L. (1999) *Biochemistry* **38,** 3393–3400
32. Jogl, G., Tao, X., Xu, Y., and Tong, L. (2001) *Acta Crystallogr. Sect. D* **57**, 1127–1134
33. Wilson, N. A., Barbar, E., Fuchs, J. A., and Woodward, C. (1995) *Biochemistry* **34,** 8931–8939
34. Fry, D. C., Fox, T. L., Lane, M. D., and Mildvan, A. S. (1985) *J. Am. Chem. Soc.* **107,** 7659–7665
35. Sloane, V., and Waldrop, G. L. (2004) *J. Biol. Chem.* **279,** 15772–15778
36. Levert, K. L., Lloyd, R. B., and Waldrop, G. L. (2000) *Biochemistry* **39,** 4122–4128
37. Sloane, V., Blanchard, C. Z., Guillot, F., and Waldrop, G. L. (2001) *J. Biol. Chem.* **276,** 24991–24996
38. Cheng, D., Chu, C.-H., Chen, L., Feder, J. N., Mintier, G. A., Wu, Y., Cook, J. W., Harpel, M. R., Locke, G. A., An, Y., and Tamura, J. K. (2007) *Protein Expression Purif.* **51,** 11–21
39. Khayat, R., Batra, R., Massariol, M.-J., Lagace, L., and Tong, L. (2001) *Biochemistry* **40,** 6344–6351
40. Janiyani, K., Bordelon, T., Waldrop, G. L., and Cronan, J. E., Jr. (2001) *J. Biol. Chem.* **276,** 29864–29870
41. Artymiuk, P. J., Poirrette, A. R., Rice, D. W., and Willett, P. (1996) *Nat. Struct. Biol.* **3,** 128–132
42. Galperin, M. Y., and Koonin, E. V. (1997) *Protein Sci.* **6,** 2639–2643
43. Thoden, J. B., Holden, H. M., Wesenberg, G., Raushel, F. M., and Rayment, I. (1997) *Biochemistry* **36,** 6305–6316
44. DeLano, W. L. (2002) *The PyMOL Manual*, DeLano Scientific, San Carlos, CA